Vibrational properties of an octagonal quasicrystal

1992 J. Phys.: Condens. Matter 4 6343

(http://iopscience.iop.org/0953-8984/4/29/018)

J. Phys.: Condens. Matter 4 (1992) 6343–6354. Printed in the UK

Vibrational properties of an octagonal quasicrystal

Zhengyou Liu†, Zhehua Zhang†, Qing Jiang† and Decheng Tian‡
† Department of Physics, Wuhan University, Wuhan 430072, People's Republic of China
‡ International Centre for Material Physics, Academia Sinica, Shengyang 110015, People's Republic of China

Received 3 January 1992, in final form 9 March 1992

Abstract. The vibrational densities of states for an octagonal quasiperiodic lattice are calculated. Crossovers from phonon excitations to fracton-like excitations are found in the low-frequency parts of the spectra (this part is referred to as the continuous spectrum); meanwhile, localized vibrational modes are observed in the high-frequency parts (this part is referred to as the characteristic spectrum). The spectral features are governed by α and β, the central and non-central force constants of the Born model. For the low-frequency continuous spectrum, when α/β equals unity (isotropic model) and when α/β is not very large, a power law is satisfied in the fracton-like excitation frequency regime but, when α/β approaches infinity, the spectrum deviates from the original power law. For the high-frequency characteristic spectrum, in an isotropic situation, i.e. in the case when $\alpha/\beta = 1$, the localized mode is isolated and a gap separates it from other modes but, when there is no longer isotropy, the gap disappears.

1. Introduction

In recent years, the spectral properties of the quasiperiodic lattice have aroused much interest; undoubtedly, one major reason for this is the experiments by Schechtman *et al* [1] which show strong evidence for the existence of quasicrystals in nature. Owing to the peculiar symmetries of this kind of structure, one expects some significant features to appear in their electronic (or vibrational) spectra. Kohmoto and co-workers [2–4] have treated theoretically the one-dimensional version of quasiperiodic lattices, and Cantor-set-like electronic (or vibrational) spectra with self-similar features were found. For Penrose tiling, the two-dimensional quasiperiodic lattice with a fivefold axis, it is not so easy to obtain the eigenvalue of the Hamiltonian analytically; many numerical methods have been developed to obtain the electronic (and/or vibrational) spectra. The earliest work on the spectral properties of a two-dimensional quasiperiodic lattice was done by Choy [5] and by Odagaki and Nguyen [6]; both investigated the behaviour of s electrons, and a central peak was found in the electronic density of states. Kohmoto and Sutherland [7, 8] explain the central peak as a zero-width band of localized electronic states; furthermore, they showed the local pattern of the localized states. In addition, the vibrational density of states, as an analogue of the electronic density of states, was briefly referred to in [6–8]. Sire and Bellissard [9] investigated the electronic behaviour of the octagonal lattice; they obtained the electronic spectra and structure using the renormalization group method, but the vibrational properties of this lattice remain unknown.

0953-8984/92/296343 + 12 $04.50

In addition to the investigation of the spectral properties of a quasiperiodic lattice, the investigation of the spectral properties of fractals has recently been very active too. Since Alexander and Orbach [10] anticipated theoretically a new excitation (they referred to it as a fracton) frequency regime in the low-frequency spectra of fractal systems, many numerical methods had been used to check this in the DLA cluster [11], percolation cluster [12] and other fractal clusters. We have studied the fractal dimensionalities for different quasiperiodic lattices with a mass scaling scheme [13]; it is found that quasiperiodic lattices have integral fractal dimensionalities. For a Fibonacci chain, the dimensionality is one; for Penrose tiling and an octagonal lattice, the dimensionalities are two. By analogy with fractals, we believe that the fracton-like excitation will appear in the low-frequency part of the vibrational spectrum of a quasiperiodic lattice but much less attention has been paid to the low-frequency part of the vibrational spectrum in the past.

We perform our numerical computation on an octagonal lattice in the present work. The aim is threefold: first, we would like to check the existence of fracton-like excitations in quasiperiodic lattices; secondly, it is expected that the high-frequency spectral properties for an octagonal lattice are specific and very different from those of Penrose tiling; thirdly, we consider the vector nature of the vibrational problem (which is more realistic for an elastic system), to determine how the vector nature of the vibration influences the spectrum. In this case, the system is not isotropic, the vibrational problem cannot be incorporated into the s-electron problem, and we expect some specific features to appear in the spectrum; however, this type of problem has previously been ignored by researchers.

2. Model and method

According to the Born model [14], the potential energy of the lattice is expressed as

$$V = \tfrac{1}{2}(\alpha - \beta) \sum_{i,j}^{\mathrm{NN}} [(\boldsymbol{u}_i - \boldsymbol{u}_j)\cdot \boldsymbol{r}_{ij}]^2 + \tfrac{1}{2}\beta \sum_{i,j}^{\mathrm{NN}} |\boldsymbol{u}_i - \boldsymbol{u}_j|^2 \tag{1}$$

where $\boldsymbol{u}_i$ is the displacement of the ith site, $\boldsymbol{r}_{ij}$ is the unit vector from site i to site j, α is the bond-stretching force constant and β is the bond-bending force constant; the summation runs over all the nearest neighbours. Thus, the vector nature of the elastic forces is included naturally. When α is chosen to equal β, the system considered becomes isotropic.

We adopt the widely used recursion method of Haydock *et al* [15, 16] which offers fast computational speed and, above all, reliability.

The local vibrational density of states [11] can be expressed as

$$\rho_{\mathrm{L}}(\omega) = -(2\omega/\pi)\,\mathrm{Im}\,\langle \boldsymbol{u}_i | 1/(\omega^2 - \mathbf{W}) | \boldsymbol{u}_i \rangle = -(2\omega/\pi)\,\mathrm{Im}\,\langle \boldsymbol{u}_i | G | \boldsymbol{u}_i \rangle \tag{2}$$

where $G = 1/(\omega^2 - \mathbf{W})$ is the Green function, $\mathbf{W}$ is the dynamical matrix and $|\boldsymbol{u}_i\rangle$ is the displacement vector of site i. The global density of states following Choy [5] and Peng and Tian [11] takes the form

$$\rho_{\mathrm{G}}(\omega) = -(2\omega/\pi)\,\mathrm{Im}\,\overline{\langle \mathbf{0} | G | \mathbf{0} \rangle} \tag{3}$$

where $|\mathbf{0}\rangle$ is the initial vector whose elements are uncorrelated variables chosen from

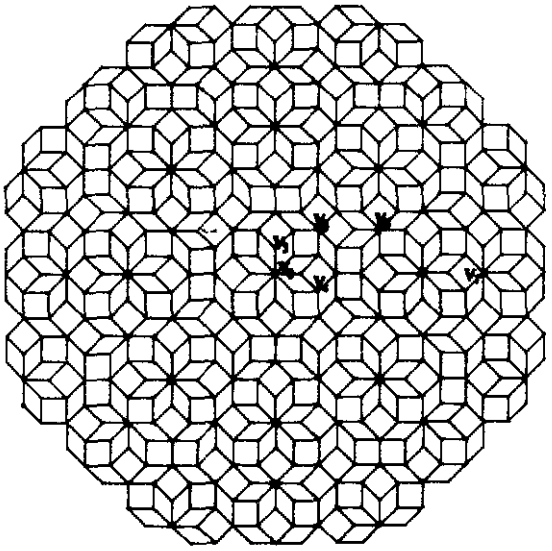

Figure 1. A portion of the octagonal lattice, where six kinds of sites are indicated by V_l ($l = 3, 4, 5, 6, 7, 8$), l representing the coordination number of the labelled site.

a Gaussian distribution with mean zero and covariance unity. In the actual calculation, ten initial vectors are chosen to obtain the average.

The octagonal lattice is a projection of a four-dimensional regular lattice onto a two-dimensional plane. The cluster used in our calculation is rather large, containing 10 457 sites; we expect that the boundary influence can be greatly reduced. Figure 1 shows a portion of our cluster; the line segments joining two sites represent bonds, and all bonds have equal lengths. The figure in fact is a tiling with eightfold symmetry. Two kinds of tile can be seen: one is a square, and the other is a rhombus with an acute angle $\pi/4$. Six kinds of local configuration can be noted; those in which the central sites are indicated by V_l ($l = 3, 4, 5, 6, 7, 8$ denoting the coordination number of the central site) are examples. In our model, all sites are occupied by the same atoms with mass unity, and the bond lengths are all taken to be equal to unity; by changing the force constants α and β, we calculate the corresponding spectra.

Under the free boundary condition, for the cluster, we calculated three series of densities of states (including global and local values), firstly with the constants $\alpha = 1$, $\beta = 0$, secondly with $\alpha = 1$, $\beta = 1$, and thirdly with $\alpha = 5$, $\beta = 1$, and also a global density of states with $\alpha = 50$, $\beta = 1$. Each spectrum can be considered to be composed of two parts: the low-frequency part is smooth and continuous, while the high-frequency part has many sharp jumps (for an integrated density of states) or sharp peaks (for the density of states). We shall refer to the two parts as the continuous spectrum and the characteristic spectrum hereafter.

3. The low-frequency continuous spectrum

Figures 2(a), 2(b), 2(c) and 2(d) show the global vibrational densities of states for the cluster with $\alpha = 1, \beta = 1$, with $\alpha = 5, \beta = 1$, with $\alpha = 50, \beta = 1$ and with $\alpha = 1, \beta = 0$,

respectively. We use a logarithmic coordinate system; the horizontal axis is the logarithm of the angular frequency of vibration, and the vertical axis is the logarithm of the global vibrational densities of states. Here, we consider only the continuous spectra, i.e. the low-frequency parts of the whole spectra. From the figure, the anomalous behaviour at low frequencies can be clearly seen near the frequency ω_c; similar anomalous behaviour in three-dimensional Penrose tiling was reported by Los and Janssen [17]. Below the frequency ω_c, the spectra are straight lines, and the slopes are unity. They correspond to typical phonon excitations, satisfying the power law $\rho_G(\omega) \propto \omega^{d_s-1}$ with $d_s = 2$. For the three cases with $\alpha = 1$, $\beta = 1$, with $\alpha = 5$, $\beta = 1$ and with $\alpha = 50$, $\beta = 1$, within a frequency region above ω_c, the spectra can be fitted as straight lines; the slopes are still unity, i.e. the spectral dimensionalities are two, exhibiting the same power law $\rho_G(\omega) \propto \omega^{d_s-1}$. Comparing the figure with the vibrational spectra for fractals, e.g. for a DLA cluster [11] and a percolation cluster [12], it can be seen that the characters of these spectra are completely similar to those for fractals. In the case of a fractal, the frequency ω_c is called the crossover frequency; below ω_c, the vibrational excitation is typical of a phonon too while, above ω_c, the vibrational excitation is due to a fracton (and no longer to a phonon!). There are two differences between the fracton and phonon [10] as follows: first, the spectral dimensionality of the fracton is different from that of the phonon, because the former depends on the fractal dimensionality of the system being considered, while the latter is a fixed integer; secondly, the vibrational state of the fracton is different from that of the phonon, because the former is usually non-extended, while the latter is always extended. As an analogue, in the case of a quasicrystal, the linear spectra above ω_c (we call ω_c the crossover frequency in this case also) should correspond to a new vibrational excitation; we introduce the term fracton-like to denote it in order to indicate the similarity between it and the fracton in the fractal system. There is a difference between the fracton-like and fracton spectral dimensionalities, which originates from the difference between the fractal dimensionalities of the fractal and the quasicrystal. For a two-dimensional fractal, the spectral dimensionality is not larger than the fractal dimensionality (which is not larger than 2) but, for a two-dimensional quasicrystal, the spectral dimensionality (see figures 2(a)–2(c)) is equal to the fractal dimensionality (which is 2 [13]). Although the fracton-like spectral dimensionality above ω_c is the same as that of a phonon below ω_c (both equal to 2), we shall see that the vibrational state for fracton-like excitation is quite different from that for the phonon in the next paragraph; this is the very reason why we need to introduce the term fracton-like to distinguish the new excitation from phonon excitation. From the above result and according to $d_s = 2d_f/d_w$ [10], one can obtain the random-walk dimensionality $d_w = 2$, for $\langle r^2 \rangle \simeq t^{2/d_w} = t$; there is no anomalous diffusive behaviour. When α/β approaches infinity the spectrum in the frequency region becomes flat (see figure 2(d)). The deviation from the original power law results from the influence of the anisotropic force. A similar result was found in the percolation model [18] and the DLA model [11].

It is interesting to examine the vibrational states in the fracton-like excitation frequency regime. Figure 3 shows the local densities of states in the low-frequency part for sites V_3–V_8 with force constants $\alpha = 1$, $\beta = 1$. Below ω_c, the densities remain the same, independent of the sites, which indicates that the phonon states are extended but, above ω_c, the densities depend on the sites, which suggests that fracton-like excitations are neither extended nor localized (see the arguments about vibrational states in the next section).

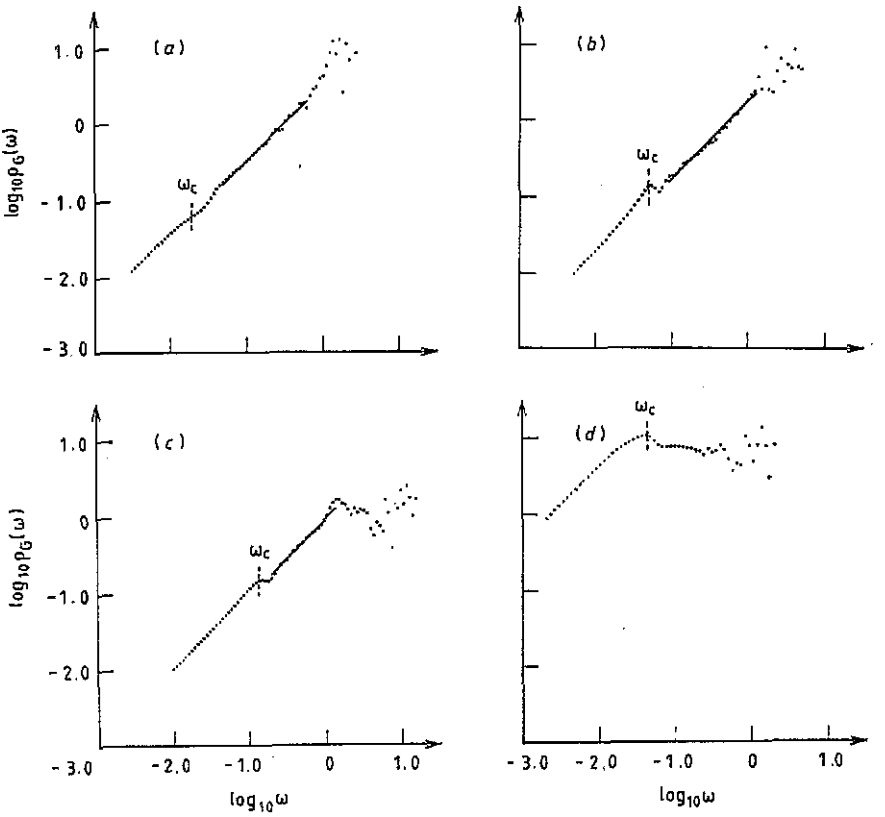

Figure 2. The vibrational densities of states for the octagonal lattice with the following constants: (a) $\alpha = \beta = 1$; (b) $\alpha = 5, \beta = 1$; (c) $\alpha = 50, \beta = 1$; (d) $\alpha = 1, \beta = 0$. The crossovers are indicated.

4. The high-frequency characteristic spectrum

Now, let us concentrate on the characteristic spectrum, which implies characteristics related to the structure of the octagonal lattice. Figure 4 shows the integrated densities $\rho'(\omega)$ of states of the system with $\alpha = 1$, $\beta = 1$. Figure 4(a) shows the global density $\rho'_G(\omega)$ of states and figures 4(b)–4(g) show the local densities of states for six different kinds of site: V_8, V_3–V_7. Figures 5 and 6 are similar to figure 4, but with $\alpha = 5$, $\beta = 1$ and with $\alpha = 1$, $\beta = 0$, respectively. Comparing figure 4 with figure 5 and figure 6, we find that the global structures of the corresponding spectra are similar. Let us examine figure 4 first. We can find some small steps in $\rho'_G(\omega)$ (see figure 4(a)) which are specified in the figure. This means that there exist some degenerate vibrational modes at these specific frequencies. Comparing $\rho'_G(\omega)$ (figure 4(a)) with $\rho'_L(\omega)$ (figures 4(b)–4(g)), we can see that these steps originate from the larger steps in the different $\rho'_L(\omega)$. The large steps in a given local spectrum indicate that the corresponding vibrational modes are favoured by the special local configuration; so they are degenerate. For example, mode $\omega_3(1)$ and $\omega_3(2)$ are favoured at site V_3, ω_7 is favoured at V_7, and eigenmode $\omega_8 = 3.05$ is absolutely dominant at V_8. There exists a simple relation between the frequency of a vibrational mode favoured by a certain site and the coordination number of the site; the larger the coordination number, the higher is the frequency or, to express it in another

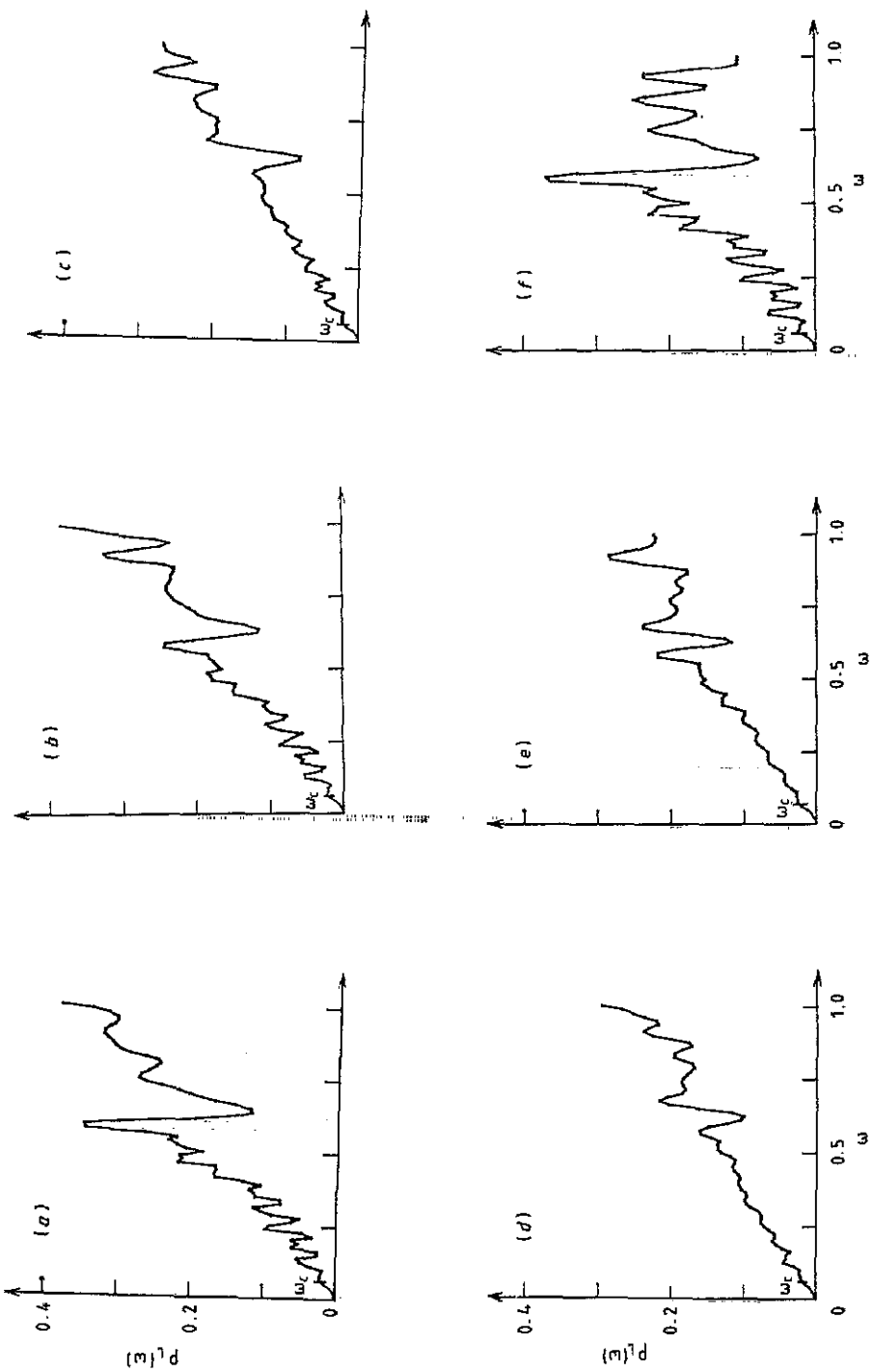

Figure 3. Local densities of states (a) for V_3, (b) for V_4, (c) for V_5, (d) for V_6, (e) for V_7 and (f) for V_8, with $\alpha = \beta = 1$. This shows that the vibrational states of fracton-like excitations are critical.

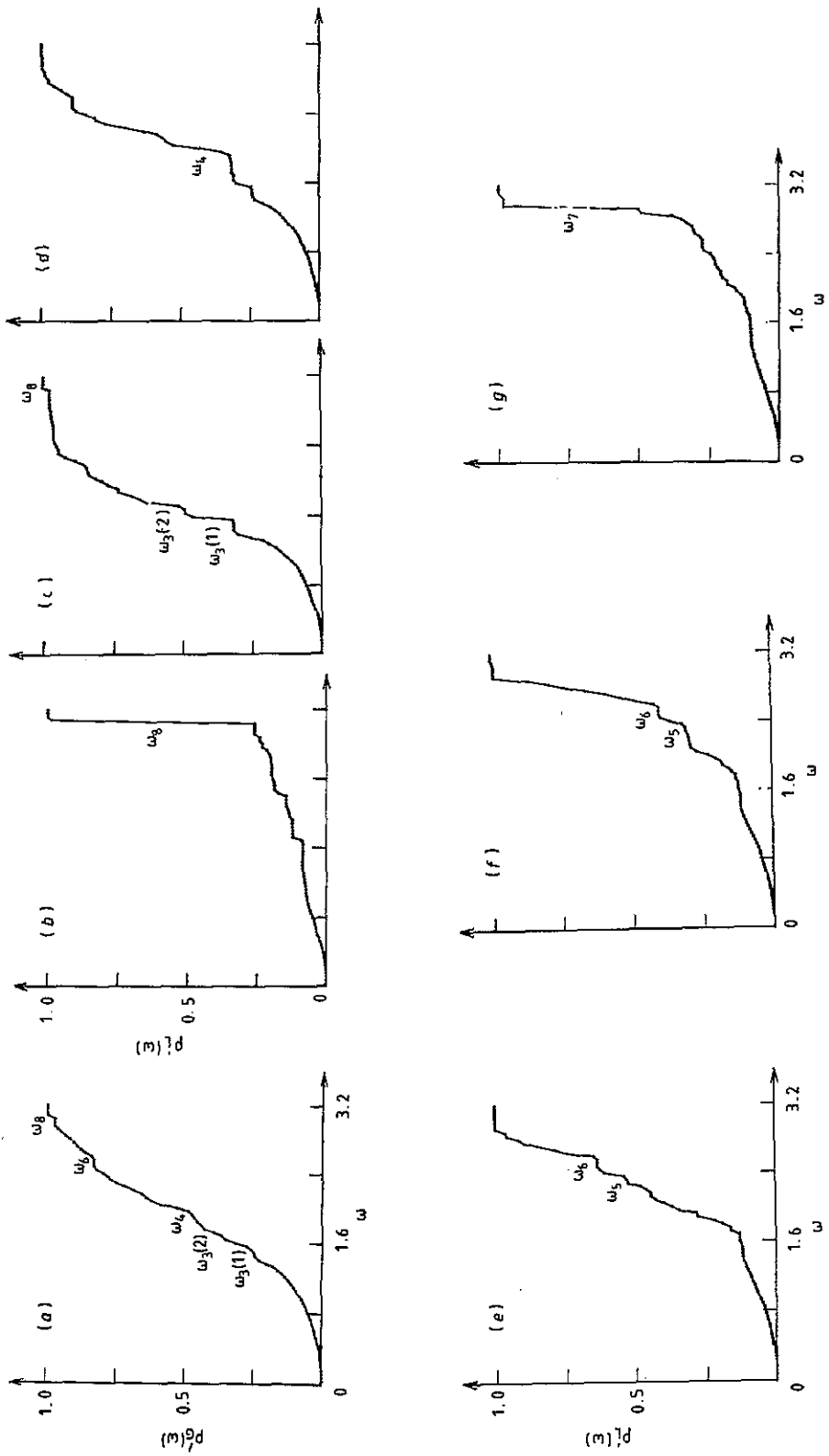

Figure 4. Integrated densities of states with constants $\alpha = \beta = 1$: (a) global density of states; (b)–(g) local densities of states for (b) V_8, (c) V_3, (d) V_4, (e) V_5, (f) V_6 and (g) V_7 sites.

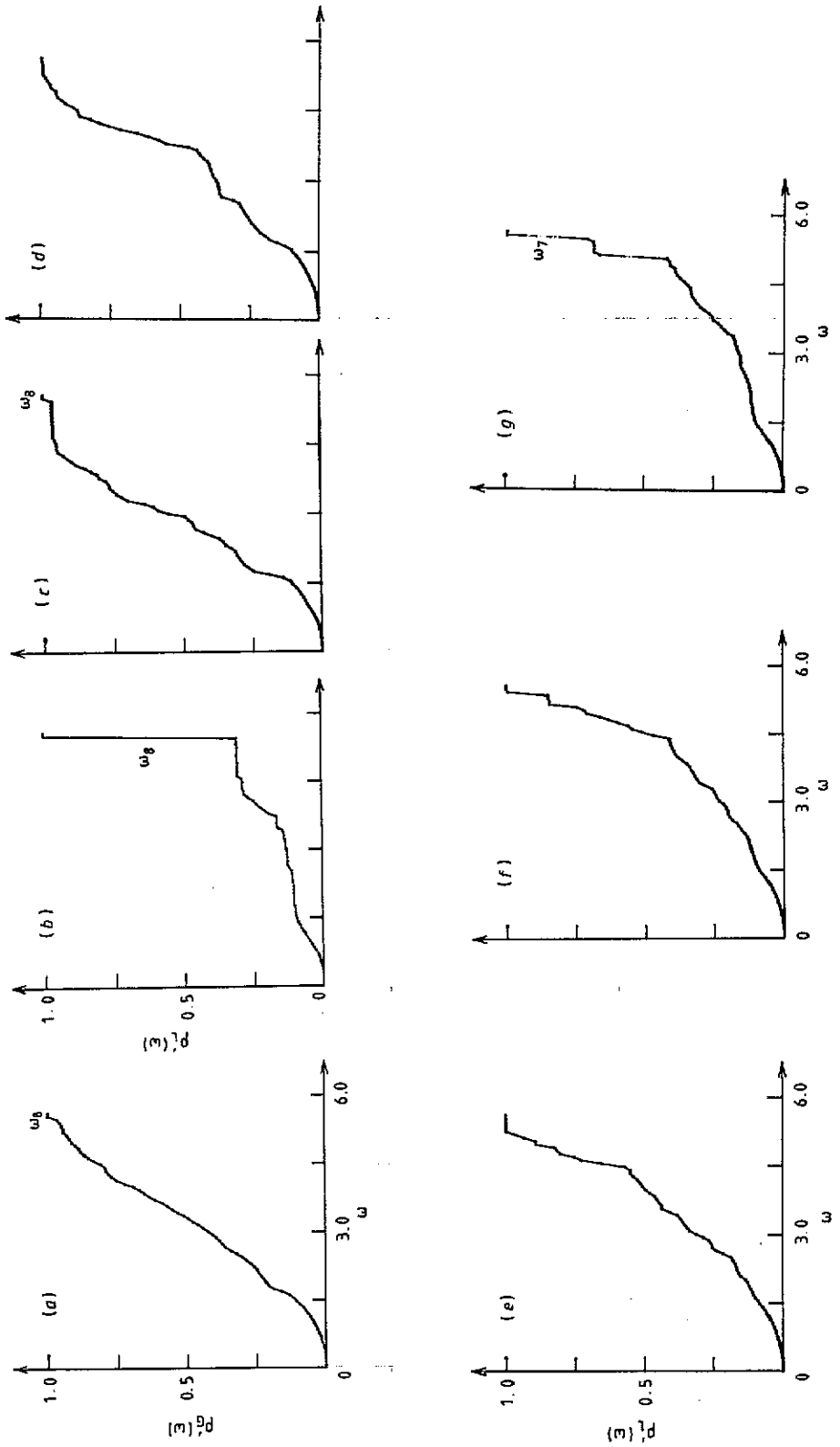

Figure 5. Similar to figure 4, but with the constants $\alpha = 5, \beta = 1$.

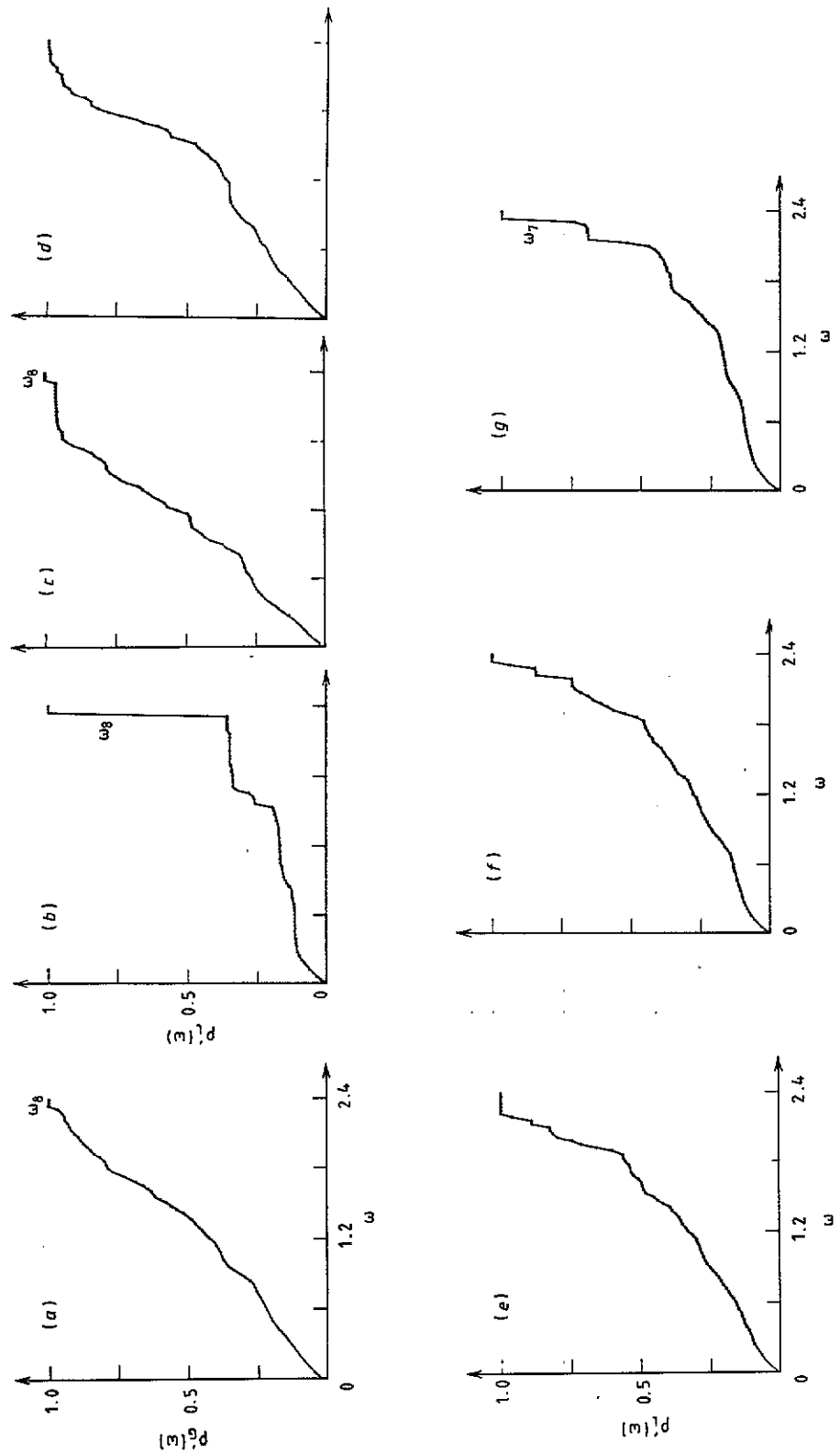

Figure 6. Similar to figure 4 and figure 5, but with the constants $\alpha = 1, \beta = 0$.

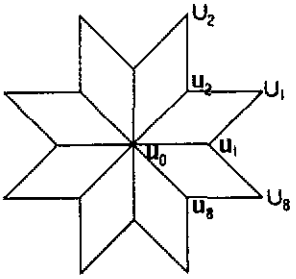

Figure 7. The local configuration of site V_8 to its second-nearest neighbours.

way, the denser the local configuration, the higher is the frequency of the mode that it favours.

From these local spectra (figures 4(b)–4(g)), we can, furthermore, obtain information about the vibrational states of these specific modes. There exist three states for the vibrational modes.

(1) If all the local densities of states for all the sites in the cluster are the same for a certain vibrational mode, the mode is extended.

(2) For a given mode, if the local densities of states for the sites in an area are not zero but become zero for the sites beyond the area, the mode is localized at the area.

(3) If both the conditions above cannot be satisfied, the vibrational mode is neither extended nor localized; the state is called critical.

According to these arguments, all the specific modes should be critical except the highest-frequency mode ω_8, which is localized.

Let us examine mode ω_8 carefully. It produces a sharp jump at ω_8 in the local density of states for site V_8 (figure 4(b)); so the mode has a much larger amplitude at the site. Comparing the local density of states for site V_8 with those for its nearest neighbour V_3 (figure 4(c)), second-nearest neighbour V_4 (figure 4(d)) and third-nearest neighbour V_5 (figure 4(e)), we find that the jumps at ω_8 decay to zero rapidly from V_8 to V_5; this means that the amplitude of mode ω_8 attenuates to zero at the third-nearest neighbour, and thus the mode is highly localized, with a localized radius of about $\sqrt{2}+1$. Mode ω_8 is not only localized but also an isolated state in the frequency space. At both sides of ω_8, within a range of frequencies, $\rho'_G(\omega)$ and all $\rho'_L(\omega)$ are flat, causing the densities of states to fall to zero; so there exists a frequency gap at the left-hand side of ω_8 (in fact, the gap width is $\omega_8 - \omega_7$), isolating mode ω_8 from the modes below ω_8, while ω_8 is the highest-frequency mode.

We can make an approximate calculation for ω_8 under the isotropic model. Figure 7 shows the local configuration of site V_8 to its second-nearest neighbours. When $\alpha = \beta$, equation (1) gives the isotropic potential

$$V = \tfrac{1}{2}\sum_{i,j}^{\mathrm{NN}} \alpha |u_i - u_j|^2. \tag{4}$$

Under the potential, the vector problem becomes a simple scalar problem; we can remove the vector notation for u. With $|u_0\rangle$ representing the displacement of site V_8,

$|u_i\rangle$ ($i = 1, 2, \ldots, 8$) the displacements of its eight nearest neighbours and $|U_I\rangle$ ($I = 1, 2, \ldots, 8$) the displacements of its second-nearest neighbours, we have

$$m\frac{\partial^2}{\partial^2 t}|u_0\rangle = \sum_{i=1}^{8}(|u_0\rangle - |u_i\rangle). \tag{5}$$

Let $|u_0\rangle = |u_a\rangle \exp(i\omega t)$; we get

$$\phi|u_0\rangle = 8|u_0\rangle - \sum_{i=1}^{8}|u_i\rangle \tag{6}$$

where $\phi = m\omega^2/\alpha$. For eight nearest neighbours, we have

$$\begin{aligned}
\phi|u_1\rangle &= 3|u_1\rangle - |u_0\rangle - |U_1\rangle - |U_8\rangle \\
\phi|u_2\rangle &= 3|u_2\rangle - |u_0\rangle - |U_1\rangle - |U_2\rangle \\
&\vdots \\
\phi|u_8\rangle &= 3|u_8\rangle - |u_0\rangle - |U_7\rangle - |U_8\rangle.
\end{aligned} \tag{7}$$

From equations (6) and (7), extracting the $|u_i\rangle$ and inserting them in equation (6), we get a relation between $|u_0\rangle$ and $|U_I\rangle$:

$$\left(4\phi - \frac{\phi(\phi-3)}{2}\right)|u_0\rangle = 8|u_0\rangle - \sum_{I=1}^{8}|U_I\rangle. \tag{8}$$

Because mode ω_0 is highly localized, $|U_I\rangle$ is much smaller than $|u_0\rangle$; ignoring $|U_I\rangle$, approximately we have

$$4\phi - \phi(\phi-3)/2 = 8. \tag{9}$$

The equation gives two roots: the reasonable root is $\phi = 9.3$, or $m\omega^2/\alpha = 9.3$. Let $m = 1$, $\alpha = 1$; according to our model, we get $\omega = 3.05$, which agrees with our numerical result $\omega_8 = 3.05$ excellently.

Although the structures in figure 4, figure 5 and figure 6 are similar, there are differences between them. When α/β increases from unity, the gap exhibited very clearly in the case of $\alpha = \beta$ (figure 4) becomes so small that it cannot be recognized any longer (see figures 5 and 6). Thus, mode ω_8 is not isolated now, but it is still localized. Figures 5(b)–5(e) and figures 6(b)–6(e) show the result evidently. With a simple calculation, we find that mode ω_8 in all cases is superlocalized, and its eigenfunction $\sim \exp(-\lambda r^\gamma)$, with $\lambda > 1$ and $\gamma > 2$.

5. Conclusions

The vibrational densities of states for an octagonal quasiperiodic lattice with varying force constants are calculated. Crossovers from phonons to fracton-like excitations, which appear to be the anomalous behaviours at low frequencies found by Los and Janssen [18] in three-dimensional Penrose tiling, are found in the low-frequency regime of these spectra. The spectral features in the fracton-like excitation frequency regime depend on the force constants α and β; when $\alpha/\beta = 1$ and when α/β is not very large, the spectrum satisfies a power law $\rho(\omega) \propto \omega^{d_s - 1}$ with $d_s = 2$ but, when α/β approaches infinity, it deviates from the power law. In the high-frequency regime, some specific

vibrational modes which are degenerate are exhibited; they are relevant to the six kinds of local configuration. They are critical except for the highest-frequency mode, which is rigorously localized in a small area with an eightfold symmetric axis. The result is different from that for Penrose tiling; the vibrational spectrum for the Penrose lattice shows only a localized mode at the centre of the spectrum. For the isotropic model, the highest-frequency mode is isolated and a frequency gap is found but, when there is no longer isotropy, i.e. when $\alpha/\beta \neq 1$, the frequency gap disappears.

Acknowledgments

The authors enjoyed the useful discussions with Dr G Peng and J Li and the assistance of L Wang and Z Yang. Some of the calculations were performed at the International Center for Theoretical Physics (ICTP), Trieste. Thanks are due to the ICTP for offering one of the authors, Z Liu, the chance to visit. Support from the PhD Foundation provided by the National Committee of Education of China and the National Science Foundation of China are acknowledged.

References

[1] Schechtman D, Blech I, Gratias D and Cahn J W 1984 *Phys. Rev. Lett.* **53** 1951
[2] Kohmoto M and Banavar J R 1986 *Phys. Rev.* B **34** 563
[3] Kohmoto M, Kadanoff P and Tang C 1983 *Phys. Rev. Lett.* **50** 1870
[4] Kohmoto M and Oono Y 1984 *Phys. Lett.* **102A** 145
[5] Choy T C 1985 *Phys. Rev. Lett.* **55** 2915
[6] Odagaki Y and Nguyen D 1986 *Phys. Rev.* B **33** 2184
[7] Kohmoto M and Sutherland B 1986 *Phys. Rev. Lett.* **56** 2740
[8] Kohmoto M and Sutherland B 1986 *Phys. Rev.* B **34** 3849
[9] Sire C 1989 *Europhys. Lett.* **10** 483
Sire C and Bellissard J 1990 *Europhys. Lett.* **11** 439
[10] Alexander S and Orbach R 1983 *J. Physique Lett.* **43** L625
Rammal R and Toulouse G 1983 *J. Physique Lett.* **44** L13
[11] Peng G and Tian D 1991 *J. Phys.: Condens. Matter* **3** 1065
[12] Yakabo K and Nakayama T 1989 *Phys. Rev.* B **40** 517
[13] Liu Z and Tian D 1991 unpublished
[14] Born M and Huang K 1954 *Dynamical Theory of Crystal Lattices* (London: Oxford University Press)
[15] Haydock R, Heine V and Kelly M 1972 *J. Phys. C: Solid State Phys.* **5** 2845
[16] Haydock R, Heine V and Kelly M 1975 *J. Phys. C: Solid State Phys.* **8** 2591
[17] Los J and Janssen T 1990 *J. Phys.: Condens. Matter* **2** 9553
[18] Feng S 1985 *Phys. Rev.* B **32** 5793